AMERICAN SOCIETY FOR MICROBIOLOGY | Journal of Virology®

GENOME REPLICATION AND REGULATION OF VIRAL GENE EXPRESSION

Construction of a Noninfectious SARS-CoV-2 Replicon for Antiviral-Drug Testing and Gene Function Studies

Hai Trong Nguyen,[a] Darryl Falzarano,[a,c] Volker Gerdts,[a,c] Qiang Liu[a,b,c]

[a]Vaccine and Infectious Disease Organization, University of Saskatchewan, Saskatoon, Saskatchewan, Canada
[b]Vaccinology and Immunotherapeutics, School of Public Health, University of Saskatchewan, Saskatoon, Saskatchewan, Canada
[c]Department of Veterinary Microbiology, Western College of Veterinary Medicine, University of Saskatchewan, Saskatoon, Saskatchewan, Canada

ABSTRACT The emerging coronavirus disease 2019 (COVID-19) outbreak caused by severe acute respiratory syndrome coronavirus 2 (SARS-CoV-2) has rapidly spread worldwide, resulting in global public health emergencies and economic crises. In the present study, a noninfectious and biosafety level 2 (BSL2)-compatible SARS-CoV-2 replicon expressing a nano luciferase (nLuc) reporter was constructed in a bacterial artificial chromosomal (BAC) vector by reverse genetics. The nLuc reporter is highly sensitive, easily quantifiable, and high throughput adaptable. Upon transfecting the SARS-CoV-2 replicon BAC plasmid DNA into Vero E6 cells, we could detect high levels of nLuc reporter activity and viral RNA transcript, suggesting the replication of the replicon. The replicon replication was further demonstrated by the findings that deleting nonstructural protein 15 or mutating its catalytic sites significantly reduced replicon replication, whereas providing the nucleocapsid protein in *trans* enhanced replicon replication in a dose-dependent manner. Finally, we showed that remdesivir, a U.S. Food and Drug Administration-approved antiviral drug, significantly inhibited the replication of the replicon, providing proof of principle for the application of our replicon as a useful tool for developing antivirals. Taken together, this study established a sensitive and BSL2-compatible reporter system in a single BAC plasmid for investigating the functions of SARS-CoV-2 proteins in viral replication and evaluating antiviral compounds. This should contribute to the global effort to combat this deadly viral pathogen.

IMPORTANCE The COVID-19 pandemic caused by SARS-CoV-2 is having a catastrophic impact on human lives. Combatting the pandemic requires effective vaccines and antiviral drugs. In the present study, we developed a SARS-CoV-2 replicon system with a sensitive and easily quantifiable reporter. Unlike studies involving infectious SARS-CoV-2 virus that must be performed in a biosafety level 3 (BSL3) facility, the replicon is noninfectious and thus can be safely used in BSL2 laboratories. The replicon will provide a valuable tool for testing antiviral drugs and studying SARS-CoV-2 biology.

KEYWORDS SARS-CoV-2, replicon, reverse genetics, nano luciferase, nonstructural protein 15, nucleocapsid protein, antivirals

Coronavirus disease 2019 (COVID-19) emerged in Wuhan, China, in December 2019, and its etiology was attributed to a novel strain of coronavirus that was named severe acute respiratory syndrome coronavirus 2 (SARS-CoV-2) (1). The disease rapidly rampaged worldwide and was declared a pandemic by the World Health Organization (WHO) in March 2020 (2). SARS-CoV-2 poses a real threat to humankind, with massive hospitalization rates and high mortality (3). As of 12 January 2021, over 88 million people had been infected, and there were more than 1.9 million deaths globally (Weekly

Citation Nguyen HT, Falzarano D, Gerdts V, Liu Q. 2021. Construction of a noninfectious SARS-CoV-2 replicon for antiviral-drug testing and gene function studies. J Virol 95:e00687-21. https://doi.org/10.1128/JVI.00687-21.

Editor Tom Gallagher, Loyola University Chicago

Address correspondence to Qiang Liu, qiang.liu@usask.ca.

Received 23 April 2021
Accepted 25 June 2021
Accepted manuscript posted online 30 June 2021
Published 25 August 2021

Epidemiological Update [WHO]). The eruption of COVID-19 has had a profound impact on the global health care network and demised the world economy (4).

SARS-CoV-2 is an enveloped positive sense RNA virus and belongs to the *Coronaviridae* family (5). Its genome size ranges from 29.8 to 29.9 kb, and the genome arrangement correlates with the basic gene features of known coronaviruses (6). The 5′-proximal two-thirds polycistronic genome comprises genes encoding viral replicase polyproteins, which are cleaved to release 16 nonstructural proteins (nsp1 to nsp16) (7) and then assemble to facilitate viral replication and transcription (8, 9). The 3′-terminal regions encode structural proteins, including spike (S), membrane (M), envelope (E), and nucleocapsid (N) (6–8), along with six accessory proteins encoded by ORF3a, ORF6, ORF7a, ORF7b, ORF8, and ORF10 (6). N is a multifunctional protein required for efficient genome replication (10) and transcription of CoV (11) in addition to its involvement in viral assembly (12). The N protein is also conserved (13), stable, and highly immunogenic (14, 15) and has therefore been proposed as one of the major targets for the development of SARS-CoV-2 therapeutics and vaccines (15–17). Nsp15, a nidoviral RNA uridylate-specific endoribonuclease (NendoU), is present in all coronaviruses (18, 19). SARS-CoV-2 nsp15 shares 88% sequence identity and 95% similarity with its known closest homolog from SARS-CoV (20). The effect of nsp15 on coronavirus RNA replication is strain specific. For instance, nsp15 is not essential for mouse hepatitis virus (MHV) and infectious bronchitis virus (IBV) replication in cell culture, although Nendo deficiency often results in impaired viral replication (21–25). However, no replication of Nendo-deficient MHV can be detected in C57BL/6 mice (21), whereas IBV with no Nendo activity replicates efficiently in embryonated chicken eggs (24), indicating various roles of nsp15 in viral replication *in vivo*. For human coronaviruses HCoV-229E and SARS-CoV, it has been shown that inactivation of Nendo activity or partial deletion of nsp15 almost completely blocks viral RNA accumulation (26–28). The effect of nsp15 Nendo enzymatic activity on the replication of SARS-CoV-2 has not been studied up until now.

Reverse genetics is a powerful approach to study viral biology. It also facilitates the generation of recombinant viruses expressing reporter genes for time- and labor-saving screening tests, generating attenuated viruses or constructing viral replicons in order to provide a safer option for studying potentially lethal infectious viruses. Recent studies have assembled the full-length viral cDNA by *in vitro* ligation (3), transformation associated recombination (TAR) (29), or cloning in a bacterial artificial chromosome (BAC) to produce transcribed RNA *in vitro* to rescue infectious SARS-CoV-2 (30). This approach has also been utilized to generate a SARS-CoV-2 replicon (31). Although considered effective, the RNA-based approach has several challenges, such as relatively poor stability of RNA molecules, technical challenges in producing viral RNA of ~30 kb in length especially when large quantities are required, relatively high costs of reagents, and technical difficulties for efficiently transfecting RNA into cultured cells. For example, instead of genome-length RNA, shorter RNA species have been shown to be the dominant transcripts after *in vitro* transcription of SARS-CoV-2 cDNA (3). In contrast, a DNA-launched BAC system has numerous advantages, including high stability, great capacity for cloning DNA from complex genomic sources, easy manipulation for large-quantity production, and the availability of multiple approaches for efficient transfection (32–34). As such, this DNA-launched platform technology has been widely employed for efficient recovery of infectious coronaviruses and construction of viral replicons (28, 35–39).

Efforts are under way to discover new specific drugs for SARS-CoV-2 (40) or repurpose existing approved drugs to bypass the time-consuming stages of novel drug development for effective treatment of COVID-19 (41). Given that SARS-CoV-2 is highly transmissible and pathogenic, all of those studies using infectious virus can only be performed in biosafety level 3 (BSL3) containment facilities, which are cumbersome. To meet the urgent need for a feasible and safer alternative to study SARS-CoV-2 and facilitate the screening for antiviral drugs for COVID-19 treatment, we constructed a

noninfectious SARS-CoV-2 replicon in a single BAC vector. Upon DNA transfection, our replicon system could replicate efficiently in cells and it was relatively easy to engineer desired mutations. The inclusion of a highly responsive nano luciferase (nLuc) reporter in our replicon makes it simple to quantitatively monitor replicon replication. By showing the effects of nsp15 and N proteins, as well as remdesivir on replicon replication, we demonstrated that our replicon should be a very useful tool for drug screening tests and gene function studies.

RESULTS

Construction and characterization of SARS-CoV-2 replicon. Following previous approaches to construct SARS-CoV replicons (28, 42, 43), we generated a subgenomic replicon BAC plasmid with all elements necessary for viral replication and nLuc-NPTII reporter-selection fusion gene driven by the TRS of the M gene (Fig. 1a). To demonstrate the replication of the replicon, Vero E6 cells were transfected with vector control, or the pSARS-CoV-2-nLuc-Rep plasmid DNA, together with an firefly luciferase (fLuc)-expressing plasmid pGL4.10. The nLuc and fLuc activities were measured at 12, 24, 48, and 72 h posttransfection (hpt). As shown in Fig. 1b and Table 1, in comparison to the vector control, the nLuc activities in replicon-transfected cells were significantly higher at all four time points. Notably, a steady increase in nLuc activities was observed from 12 to 72 h (Fig. 1b and Table 1). At the protein level, we detected the presence of the nLuc-NPTII fusion protein only in replicon-transfected cells by Western blotting (Fig. 1c). Furthermore, we measured the nucleocapsid transcript levels by RT-qPCR with N-specific primers (Fig. 1d). Our results showed replicon transfection resulted in the production of N-specific RNA transcripts that were absent in mock-transfected cells (Fig. 1d). No RT control did not show a positive amplification (Fig. 1d). To demonstrate the nucleocapsid protein at the protein level, we performed immunofluorescence staining on vector- or replicon-transfected cells using a rabbit anti-SARS-CoV-2 N protein generated in-house as the primary antibody. As shown in Fig. 1e, while there was no specific staining in vector-transfected cells, cytoplasmic staining was observed in cells transfected with the replicon, indicating the expression of the nucleocapsid protein. The cytoplasmic localization of the nucleocapsid protein is consistent with that reported recently in another study (38). These results collectively indicated that nLuc protein with enzymatic activity driven by M transcription regulatory sequence (TRS) and nucleocapsid RNA transcript driven by its TRS, as well as the nucleocapsid protein, can be detected after transfection of Vero E6 cells with our replicon. These results demonstrated that our pSARS-CoV-2-nLuc-Rep replicon is very likely capable of replicating in Vero E6 cells. A positive correlation between the viral RNA levels and the nLuc activities should allow us to utilize the latter as a convenient and sensitive biological readout for the analysis of replicon replication.

Our replicon encodes the neomycin phosphotransferase II as a fusion protein with nLuc and the fusion protein should confer resistance against neomycin selection. This will allow us to establish Vero E6 cells with autonomously replicating replicon. To do so, Vero E6 cells were transfected with the replicon construct, selected by G418, and passaged for up to 10 times at the time of submission of the manuscript. The nLuc activities were measured in cells at different passages. As shown in Fig. 1f, the nLuc activities maintained at significantly higher levels than the basal nLuc activity from passages 3 to 10, although a gradual decrease was observed. These results indicated that the replicon can replicate to a substantial level in the presence of G418 selection pressure.

The replication of the SARS-CoV-2 replicon is impaired with NendoU (nsp15) mutations. Our results thus far strongly suggested replication capability of the SARS-CoV-2 replicon. To further substantiate this conclusion, we chose to study the effect of nsp15 on replicon replication in two approaches. First, the nsp15 coding sequence was removed from the replicon, resulting in the plasmid pSARS-CoV-2-nLuc-Rep Δnsp15. Second, to specifically investigate the role of NendoU enzymatic activity of nsp15 in replicon replication, an H235A H250A-nsp15 mutant replicon was created, resulting in

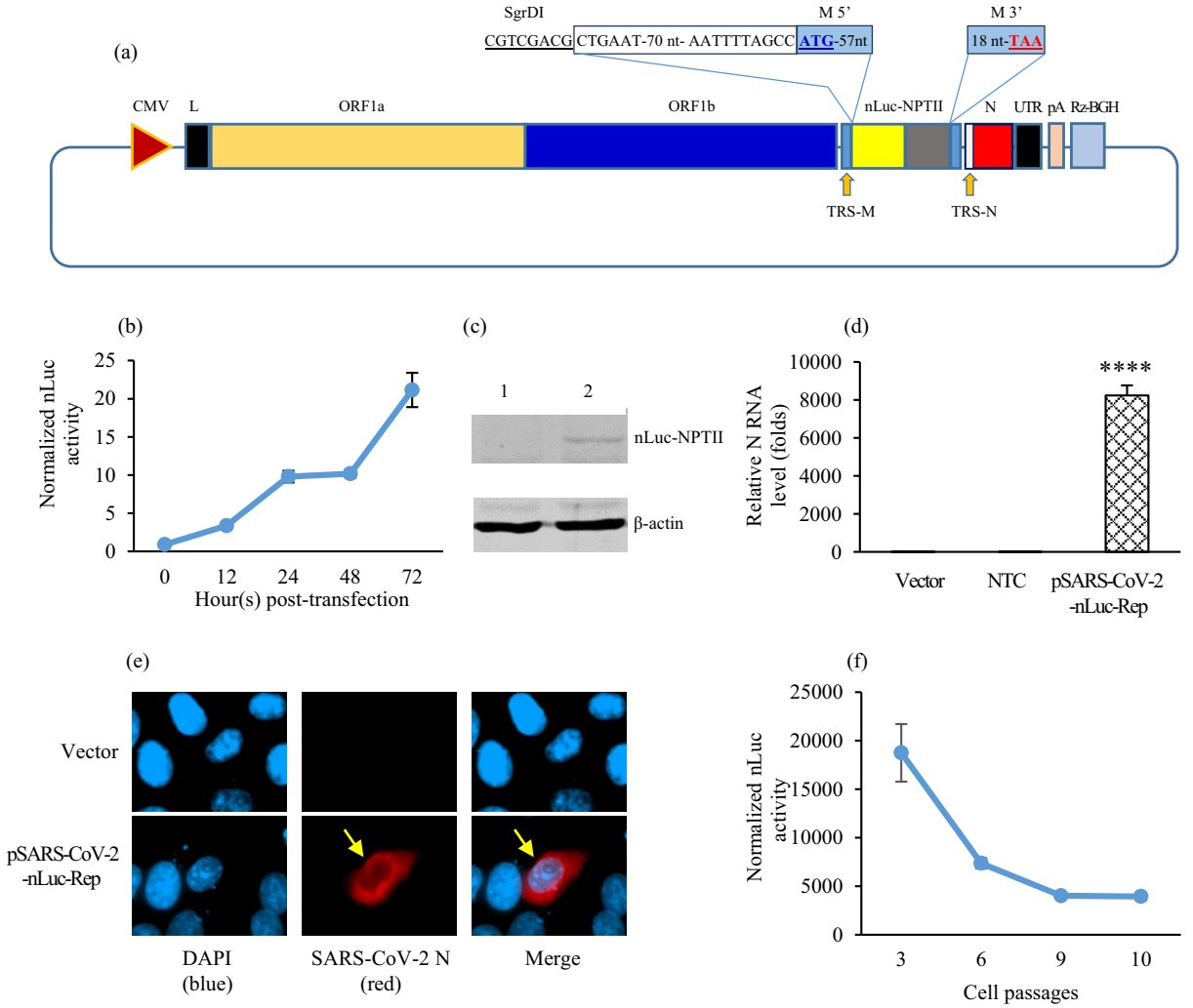

FIG 1 Construction and characterization of SARS-CoV-2 replicon. (a) Schematic diagram of the replicon construct pSARS-CoV-2-nLuc-Rep. Cytomegalovirus promoter (CMV), SARS-CoV-2 5′ leader sequence (L), replicase genes (ORF1a and -1b), nano luciferase gene (nLuc) fused with neomycin phosphotransferase II (NPTII) gene inserted downstream of the first 60 nt of M gene preceded by its transcription regulatory sequence (TRS), followed by the last 18 nt of the M gene, and the N gene, along with its TRS sequence, a poly(A) tail (pA), hepatitis delta virus ribozyme (Rz), and bovine growth hormone termination sequence (BGH) were cloned in the pSMART-BAC vector. (b) Replication kinetics of SARS-CoV-2 replicon. Vero E6 cells were cotransfected with pGL4-10(luc2) and pSARS-CoV-2-nLuc-Rep, harvested at different time points for analysis. The nano luciferase activity was measured by a luciferase assay and normalized to the firefly luciferase reading. (c) Demonstration of nLuc-NPTII fusion protein expressed in cells transfected with SARS-CoV-2 replicon construct. The expression of Flag-tagged nLuc-NPTII fusion protein was identified by Western blotting with an anti-Flag antibody. The levels of β-actin were also determined by a β-actin-specific antibody. Lanes: 1, pGL4-10(luc2) and vector cotransfection; 2, pGL4-10(luc2) and pSARS-CoV-2-nLuc-Rep cotransfection. (d and e) SARS-CoV-2 N RNA levels (d) and expression of N protein in cells transfected with the SARS-CoV-2 replicon construct (e). Vero E6 cells were harvested at 48 h after cotransfection with vector or SARS-CoV-2 replicon construct and pGL4-10(luc2). RNA levels of the N gene were determined by RT-qPCR and normalized against GAPDH levels. ****, $P < 0.0001$; NS, not significant. N protein was identified by immunofluorescent staining using an anti-SARS-CoV-2 N as the primary antibody. Cell nucleus was stained by DAPI. (f) nLuc activity in replicon-replicating cells. Vero E6 cells were transfected with SARS-CoV-2 replicon construct and selected with G418. Survival cells were subcultured and harvested at passages 3, 6, 9, and 10 for luciferase assay.

the plasmid pSARS-CoV-2-nLuc-Rep H235A H250A-nsp15 (Fig. 2a). Mutations at catalytic sites of nsp15, including H235A and H250A, have been reported to severely reduce the endoribonuclease activity (44). When the Δnsp15 replicon plasmid was transfected into Vero E6 cells, the nLuc activity was reduced significantly in comparison to that in wild-type replicon-transfected cells. Similarly, a significant reduction in nLuc activity was observed in cells transfected with the H235A H250A-nsp15 mutant replicon plasmid (Fig. 2b). To substantiate the luciferase assay results, we measured nLuc RNA levels by RT-qPCR. As shown in Fig. 2c, nLuc RNA levels were significantly decreased in cells transfected with the nsp15 mutant replicons in comparison to wild-

TABLE 1 nLuc activities in Vero E6 cells after pSARS-CoV-2-nLuc-NPTII replicon transfection

	Activity	
Sampling time (hpt)	Nluc (pSARS-CoV-2-nLuc-NPTII)	fLuc (pGL4.10)
0	186	221
	250	218
	213	219
12	25,795	6,422
	16,796	6,412
	19,257	6,065
24	74,088	7,974
	66,798	7,707
	75,000	8,005
48	88,472	8,416
	86,457	8,496
	81,797	9,034
72	166,368	7,952
	143,971	7,908
	152,088	8,364

type replicon transfection, correlating with the nLuc readings (Fig. 2b). Taken together, these results showed an important role of nsp15 Nendo activity in SARS-CoV-2 replication. They also demonstrated that the nLuc signal detected is indeed due to viral RNA replication.

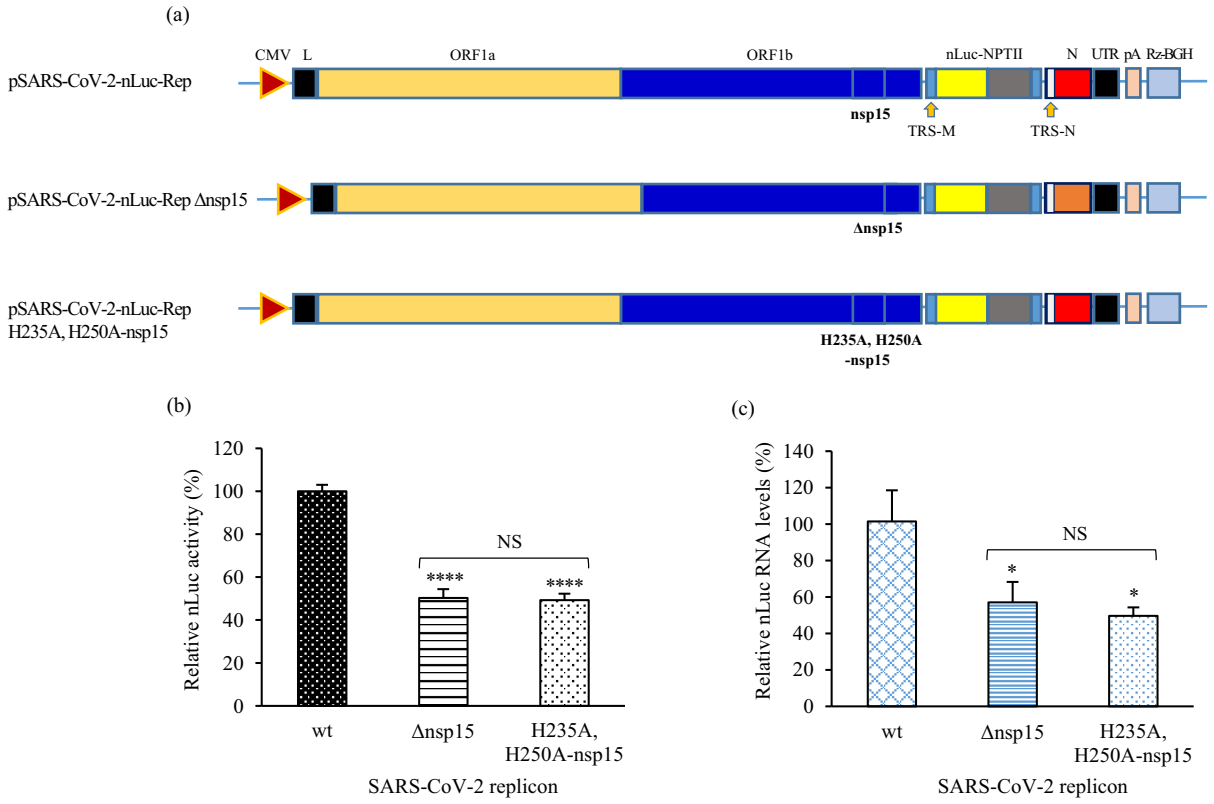

FIG 2 Nsp15 mutants reduce the replication of SARS-CoV-2 replicon. (a) Schematic diagram of SARS-CoV-2 replicon wt, Δnsp15, and H235A, H250A-nsp15 constructs. (b and c) Nano luciferase activity analysis by luciferase assay (b) and nLuc RNA levels determined by RT-qPCR (c). Vero cells were cotransfected with 250 ng of pGL4-10(luc2) as an internal control and 250 ng of pSARS-CoV-2-nLuc-Rep, pSARS-CoV-2-nLuc-Rep Δnsp15, or pSARS-CoV-2-nLuc-Rep H235A, H250A-nsp15 constructs. At 48 hpt, the cells were harvested for luciferase assay (b) and RT-qPCR (c). The average nano luciferase value and RNA level obtained from pSARS-CoV-2-nLuc-Rep (wt)-transfected cells was set to 100%. *, $P < 0.05$; ****, $P < 0.0001$; NS, not significant. The luciferase assay experiment was performed twice with similar results.

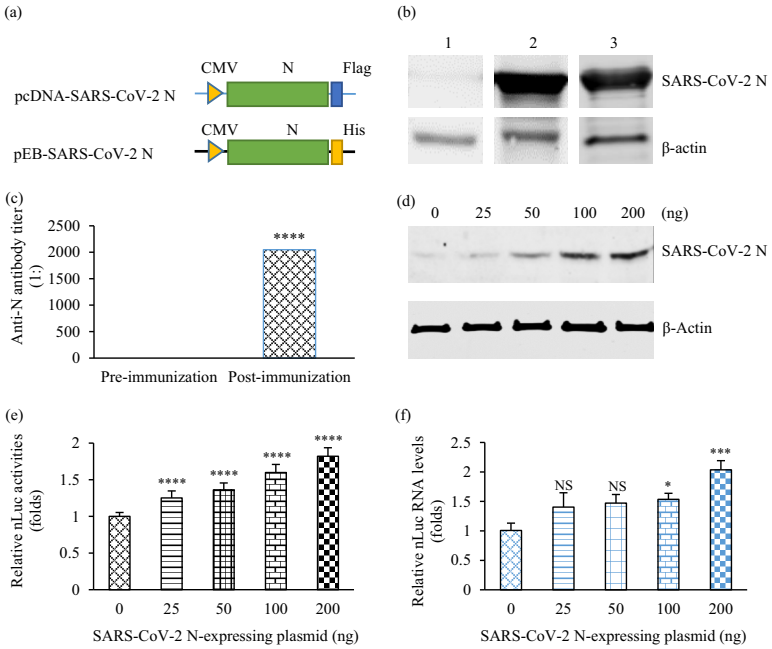

FIG 3 Generation of SARS-CoV-2 N antisera and the effect of N protein on SARS-CoV-2 replicon replication in *trans*. (a) Schematic representations of SARS-CoV-2 N in constructed plasmids for immunization and cell line establishment. (b) Western blotting for identification of N protein expressed in HEK293 cells transfected with the pcDNA-SARS-CoV-2 N plasmid and in SARS-CoV-2 N-expressing cells after pEB-SARS-CoV-2 N transfection and puromycin selection. Lanes: 1, vector-transfected cell lysate; 2, pcDNA-SARS-CoV-2 N-transfected cell lysate; 3, SARS-CoV-2 N-expressing cell lysate. (c) Titers of antibodies against SARS-CoV-2 N protein in rabbit pre- and postimmunization sera as determined by ELISA. (d) Expression of SARS-CoV-2 N protein identified by Western blotting with our anti-N polyclonal antibody. The levels of β-actin were determined by using an anti-β-actin antibody. (e and f) N protein enhances SARS-CoV-2 replicon replication determined by luciferase assay (e) and RT-qPCR (f). Vero E6 were cotransfected with 100 ng of pSARS-CoV-2-nLuc-Rep construct, 100 ng of pGL4-10(luc2) vector as an internal control, and 0, 25, 50, 100, or 200 ng of the plasmid expressing SARS-CoV-2 N protein (pcDNA-SARS-CoV-2 N) or enhanced green fluorescent protein (pcDNA-EGFP) to keep the total amounts of DNA used for transfection constant. Nano luciferase activities and RNA levels were determined at 48 hpt by a luciferase assay and RT-qPCR, respectively. The average nano luciferase value and RNA level obtained from cells transfected with 0 ng of SARS-CoV-2 N-expressing plasmid was set to 1. *, $P < 0.05$; ***, $P < 0.001$; ****, $P < 0.0001$; NS, not significant.

Nucleocapsid protein enhances the replication of SARS-CoV-2 replicon in a dose-dependent manner. The N protein has been shown to play an important role in the coronavirus life cycle, including viral transcription and replication (45). To demonstrate the feasibility of using our replicon model to study the role of SARS-CoV-2 N protein in viral replication, we quantified the replication of our replicon upon providing the N protein in *trans*. We constructed plasmids either transiently or stably expressing the SARS-CoV-2 N with a Flag or polyhistidine tag (Fig. 3a). Using tag-specific antibodies, we demonstrated N protein expression in HEK293 cells by Western blotting (Fig. 2b). To specifically detect the N protein, we generated a polyclonal antibody against the SARS-CoV-2 N protein using a DNA prime-protein boost strategy as outlined in Materials and Methods. The titer of the polyclonal antibody was 1:2,048, as determined by enzyme-linked immunosorbent assay (ELISA) (Fig. 3c).

Next, we studied the effects of N protein on the replication of SARS-CoV-2 replicon. For this purpose, the SARS-CoV-2 nLuc replicon was cotransfected with increasing amounts of a plasmid-expressing SARS-CoV-2 N protein into Vero E6 cells, and the replication was measured by determining the luciferase activity, as well as by RT-qPCR. Results from both assays showed that expression of the N protein in *trans* significantly enhanced the replication of our replicon in a dose-dependent manner (Fig. 3e and f). N protein expression was demonstrated in Western blotting (Fig. 3d). These results once again demonstrated the replication of our SARS-CoV-2 replicon. They also indicated

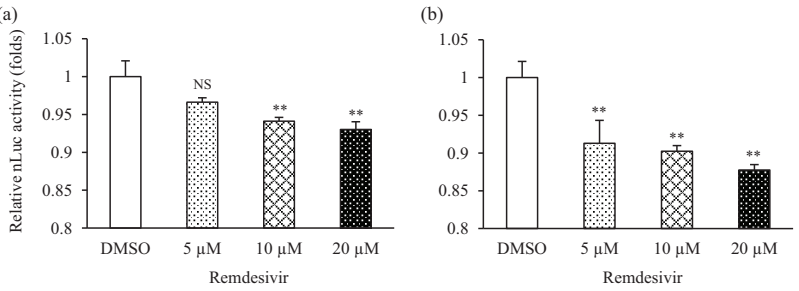

FIG 4 Inhibition of SARS-CoV-2 replicon replication by remdesivir. Vero E6 cells were cotransfected with 250 ng of pSARS-CoV-2-nLuc-Rep replicon, and 250 ng of pGL4.10. At 12 hpt, cells were treated with 5, 10, or 20 μM remdesivir or the same volume of diluent DMSO. Cells were harvested at 24 h (a) or 48 h (b) after treatment for nano luciferase analysis. The average nano luciferase value obtained from DMSO-treated cells was set to 1. **, $P < 0.01$; NS, not significant.

that the nucleocapsid protein enhances viral replication in a dose-dependent manner when expressed in *trans*.

Remdesivir inhibits the replication of SARS-CoV-2 replicon. To explore the feasibility of using the replicon system as a drug-screening tool, an inhibition assay was performed using remdesivir, a U.S. Food and Drug Administration (FDA)-approved antiviral drug that has been evaluated in the context of SARS-CoV-2 infection in tissue culture and animal models, as well as COVID-19 patients (46, 47). To determine the effect of remdesivir on the replication of our replicon, Vero E6 cells transfected with the SARS-CoV-2 nLuc replicon were treated with 5, 10, or 20 μM remdesivir for 24 or 48 h before nLuc activities were measured. Results showed that nLuc activities in SARS-CoV-2 replicon-replicating cells treated with 5 μM remdesivir were significantly reduced in comparison to dimethyl sulfoxide (DMSO) control after 48 h, while the reduction is not statistically significant after 24 h of the treatment. A slightly further reduction of the nLuc activity was observed after treatment with remdesivir at 10 μM, and the inhibitory effect was more pronounced when 20 μM remdesivir was used (Fig. 4). It is worth noting that no cytotoxic effect was observed in the treated cells at all concentrations. These results indicated that remdesivir can inhibit the replication of our SARS-CoV-2 replicon, consistent with previous studies. These results also suggested that our replicon can be a reliable and sensitive system for antiviral development.

DISCUSSION

Facilitating antiviral research, therapeutic production, and gene functional studies are some of the key advantages of a viral replicon system, especially for such a deadly virus as SARS-CoV-2. In this study, we developed a noninfectious and DNA-launched SARS-CoV-2 reporter replicon. The SARS-CoV-2-nLuc replicon allows utilizing nano luciferase as a reliable and rapid readout for viral replication. Nano luciferase can emit luminescence that is linearly proportional over a 1,000,000-fold concentration range (Promega.ca), thereby providing a highly sensitive, and less labor-intensive means than the conventional virological assays, such as virus titration. Another feature of the replicon is that, without the spike, envelope and membrane proteins, no infectious virus can be generated, and thus the replicon can be safely and conveniently manipulated in a BSL2 laboratory instead of a BSL3 facility, a prohibitory requirement for many researchers.

Coronavirus nsp15 is a uridylate-specific endoribonuclease with a C-terminal catalytic domain belonging to the EndoU family (20). Nsp15 was proposed to affect viral replication by interfering with the innate immune response (23) and evasion of host pattern recognition (48). Nsp15 is also highly conserved and thought to be involved in coronavirus biology and thus a candidate as a drug target (49, 50). Given the various effects of nsp15 on coronavirus replication as discussed earlier, it becomes necessary to study the nsp15 of each coronavirus. Our investigation found that deletion of nsp15

or mutations of its catalytic sites significantly impairs the replication ability of the SARS-CoV-2 replicon. These results, for the first time, demonstrate the importance of nsp15 for SARS-CoV-2 replication. In addition, overexpression of the N protein in *trans* enhanced replication of the replicon in a dose-dependent manner. These findings not only established the replication capability of our SARS-CoV-2 replicon but also underscored the feasibility of using our replicon to study the functions of a viral protein either in *cis* or in *trans*.

While vaccines against SARS-CoV-2 are being very actively developed, repositioning of existing drugs and developing new virus-specific therapeutics are also a critical part of our response to the COVID-19 pandemic. A quick, sensitive, and BSL2-compatible system with a high-throughput adaptable reporter for measuring viral replication should significantly accelerate antiviral evaluation. Luciferase is often chosen as a suitable reporter gene for this purpose (51). Remdesivir is a 1′-cyano-substituted analog of adenosine that has a documented capacity of inhibiting human coronaviruses SARS-CoV, MERS-CoV, and SARS-CoV-2 (52–54). As proof of principle, we showed an inhibitory effect of remdesivir on the replication of our SARS-CoV-2 replicon. These results indicated that our replicon could be a very useful system in antiviral development for SARS-CoV-2.

In conclusion, we have established a DNA-launched, BSL2-compatible subgenomic SARS-CoV-2 nLuc reporter replicon. This reverse-genetics system can be an important tool for studying viral replication and protein functions. The replicon containing the nano luciferase reporter with a high-throughput potential should also be very useful for antiviral drug discovery.

MATERIALS AND METHODS

Plasmid construction. To enable genetic manipulation of the SARS-CoV-2 genome, four fragments covering the full genome of SARS-CoV-2 strain Wuhan-Hu-1 (GenBank accession number NC_045512) were synthesized and cloned in pUC57 vector (Bio Basic). These fragments were F1 (nucleotides [nt] 1 to 8605), F2 (nt 8598 to 15049), F3 (nt 15050 to 22233), and F4 (nt 22227 to 29903). Subsequently, the cytomegalovirus (CMV) promoter was amplified from the pcDNA3.1(+) vector (Thermo Fisher Scientific) by PCR with pSMART(AscI)-CVM-F and 3903(PmlI, PmeI)-R primers. Similarly, hepatitis delta virus ribozyme (Rz), bovine growth hormone (BGH) polyadenylation, and terminator sequences were amplified from plasmid pBAC-TGEV^{FL} (kindly provided by Luis Enjuanes) with 3903(PmlI)-F and pSMART(NotI)-HDVRz-R primers. The two amplified products were then cloned into the BAC vector pSMART-BAC (Lucigen), amplified by PCR with pSMART(NotI)-F and pSMART(AscI)-CVM-R primers, to generate an intermediate plasmid pSMART-CMV-Rz-BGH.

To generate a cDNA clone for SARS-CoV-2, six overlapping fragments were amplified separately by PCR with six pairs of primers: CMV-Wh_1-F/3408-R, 3240-F/8622-R, 8577-F/15075-R, 15022-F/22252-R, and 22203-F/29875-R. Subsequently, a full-length SARS-CoV-2 cDNA clone was constructed by assembling the six cDNA fragments into pSMART-CMV-Rz-BGH and designated pSARS-CoV-2 Fl. A subgenomic SARS-CoV-2 replicon clone was generated following the strategy previously described for the construction of a SARS-CoV replicon (28). Specifically, two cDNA fragments amplified by PCR with the primers 20076_F/21623 SgrDI_R and 28131 SgrDI_F/HDVRz-R2 were assembled into pSARS-CoV-2 Fl digested with BstBI and RsrII to generate a SARS-CoV-2 cDNA replicon construct (pSARS-CoV-2-Rep) carrying sequences that are necessary for coronavirus replication, including the 5′ and 3′ untranslated regions, the replicase genes, and the nucleocapsid (N) gene. An SgrDI restriction site was introduced between the replicase coding sequences and the TRS for N gene for subsequent insertion of a reporter gene and/or a selection marker. To construct a SARS-CoV-2 replicon with a sensitive reporter gene and selection potential, a cassette containing TRS for the membrane (M) protein, the first 60 nt of the M gene, the coding sequence for Flag-tagged nLuc-neomycin phosphotransferase II (NPTII) fusion protein, and the last 18 nt of the M gene was generated by overlapping extension PCR with the primers 21623_26437-F/26582_3xFlag-R; 26582_3xFlag-F/nLuc_NPTII-R; nLuc_NPTII-F/28131_NTPII-R; and 28131_R2 and cloned into pSARS-CoV-2-Rep at SgrDI site to generate pSARS-CoV-2-nLuc-Rep. A Δnsp15 replicon construct was generated by assembling three DNA fragments, amplified separately by PCR from pSARS-CoV-2-nLuc-Rep plasmid with the primers 18084_F and 19596_20659_R; 19596_20659_F and 26582_3xFlag_R; and 21623_26437_F and 28131_R2 into the pSARS-CoV-2-nLuc-Rep digested with Bsu36I and SgrDI to obtain pSARS-CoV-2-nLuc-Rep Δnsp15. An nsp15 H235A, H250A mutant replicon construct was created by assembling two DNA fragments, amplified separately by PCR from pSARS-CoV-2-nLuc-Rep plasmid with the primers 20283_20377-F, 26582_3xFlag-R; 21623_26437-F and 28131-R2, into the pSARS-CoV-2-nLuc-Rep digested with BstBI and SgrDI to obtain pSARS-CoV-2-nLuc-Rep nsp15-H235A, H250A. Phusion High-Fidelity DNA polymerase (Thermo Fisher Scientific) was used for PCR amplification of desired DNA sequences and primers for PCR are listed in Table 2. All plasmids were constructed by GenBuilder Plus

TABLE 2 Primers for PCR amplification and RT-qPCR

Primer	Nucleotide sequence (5′–3′)	Source or reference
Cloning		
pSMART(AscI)-CMV-F	CCATGTTGGTATGAGGCGCGCCTTGACATTGATTATTGACTAGTTATTAATAG	This study
3903(PmlI, PmeI)-R	CCTAAGAAGCTATTAAAATCACGTGAAGTTTAAACCTTTAATGCCAGTAAGCAGTGGGTTCTC	This study
3903(PmlI)-F	CTTCACGTGATTTTAATAGCTTCTTAGGAGAATGACAAAAAAAAAAAAAAAAAAAAAAAAAAAAAAGG	This study
pSMART(NotI)-HDVRz-R	GGAGTCACTAGTATTTAGGTGACACTATAGAAGCGGCCGCACATGTACAGAGCTCGAGCTC	This study
pSMART(NotI)-F	GTGCGGCCGCTTCTATAGTGTCACCTA	This study
pSMART(AscI)-CMV-R	CTAGTCAATAATCAATGTCAAGGCGCGCCTCATACCAACATGGTCAAATAAAACGAAAG	This study
CMV-Wh_1-F	GGCTAACTAGAGAACCCACTGCTTACTGGCATTAAAGGTTTATACCTTCCCAGGTAACAAACCAACC	This study
3408-R	CATTTTTAATGTATACATTGTCAGTAAG	This study
3240–F	ACGGCAGTGAGGACAATCAG	This study
8622-R	GGAACACAAGTGTAACTTTAATTAACTGCTTCAACCAATTATTAAC	This study
8577-F	GTTAATAATTGGTTGAAGCAGTTAATTAAAGTTACACTTGTGTTCC	This study
15075-R	GTTATAGTAGGGATGACATTACGTTTTGTATATGCGAAAAGTGCATCTTGATCC	This study
15022-F	GGATCAAGATGCACTTTTCGCATATACAAAACGTAATGTCATCCCTACTATAAC	This study
22252-R	GGTTCTAAAGCCGAAAAACCCTGAGGGAGATCACGCACTAAATTAATAGG	This study
22203-F	CCTATTAATTTAGTGCGTGATCTCCCTCAGGGTTTTTCGGCTTTAGAACC	This study
29875-R	TTTTTTTTTTTTTTTTTTGTCATTCTCCTAAGAAGCTATTAAAATCACATGGGG	This study
20076_F	ACCATCTGTAGGTCCCAAAC	This study
21623 SgrDI-R	GGTAAACAGGAAACTGTCGTCGACGTGGTTGTAAGATTAACACACTGAC	This study
28131 SgrDI-F	GTGTGTTAATCTTACAACCACGTCGACGACAGTTTCCTGTTTACCTTTTAC	This study
HDVRz-R2	GGATCCGAGCTCTCCCTTAG	This study
21623_26437-F	CCACTAGTCTCTAGTCAGTGTGTTAATCTTACAACCACGTCGACGCTGAATTCTTCTAGAGTTCCTG	This study
26582_3xFlag-R	CGTCATGGTCTTTGTAGTCCATCCATTGTTCAAGGAGCTTTTTAAGC	This study
26582_3xFlag-F	CTTAAAAAGCTCCTTGAACAATGGATGGACTACAAAGACCATGACGG	This study
nLuc_NPTII-R	GCAATCCATCTTGTTCAATCATCGCCAGAATGCGTTCGCACAGCCG	This study
nLuc_NPTII-F	GCTGTGCGAACGCATTCTGGCGATGATTGAACAAGATGGATTGCAC	This study
28131_NTPII-R	TGTCGTCGACGCGAGATGAAACATCTGTTGTCACTTACTGTACAAGCAAAGCAATGAAGAACTCGTCAAGAAGGCG	This study
28131-R2	GTTCCTGGCAATTAATTGTAAAAGGTAAACAGGAAACTGTCGTCGACGCGAGATGAAACATCTGTTGTC	This study
18084-F	CACTGGGTTACATCCTACAC	This study
19596_20659-R	CGGTTGCCACGCTTGACTAGACTGAAGTCTTGTAAAAGTGTTCCAG	This study
19596_20659-F	CTGGAACACTTTTACAAGACTTCAGTCTAGTCAAGCGTGGCAACCG	This study
RT-qPCR		
nCoV2N-FD	CACATTGGCACCCGCAATC	55
nCoV2N-Rev	GAGGAACGAGAAGAGGCTTG	55
GAPDH-FD	AAGGTGAAGGTCGGAGTC	56
GAPDH-Rev	GGTGGAATCATACTGGAACA	56
nLuc-F	CATCATCCCGTATGAAGGTC	This study
nLuc-R	CGATTACCAGTGTGCCATAG	This study

Cloning kit (GenScript) and verified by PCR targeting the insertion junctions, restriction enzyme digestion, and DNA sequencing.

After optimization for mammalian expression, the coding sequence for SARS-CoV-2 nucleocapsid (N) protein was synthesized (Bio Basic) and cloned in-frame with a C-terminal Flag tag into an expression vector pcDNA3.1 to give rise to pcDNA3-SARS-CoV-2 N-Flag. Plasmid pcDNA3-EGFP-Flag was also generated to express Flag-tagged enhanced green fluorescent protein (EGFP). Plasmid pEB-SARS-CoV-2 N-His_{12} was generated after cloning the optimized N coding sequence in-frame with a C-terminal polyhistidine tag into an episomal vector pEB4.6 expressing the Epstein-Barr virus nuclear antigen and puromycin-resistant gene (kindly provided by Robert Brownlie).

Cells, transfection, and luciferase assay. Vero E6 and HEK293 cells were maintained in Dulbecco modified Eagle medium (Sigma-Aldrich) supplemented with 10% (vol/vol) fetal bovine serum (Sigma-Aldrich) and 100 U/ml penicillin-streptomycin (Gibco) at 37°C in 5% CO_2 atmosphere. Cells were transfected by plasmid DNA with Jet-PEI transfection reagent (Polyplus-Transfection). To establish Vero E6 cells with neomycin resistance after transfection with the pSARS-CoV-2-nLuc-NPTII replicon, cells were cultured with medium containing 1000 μg/ml of Geneticin (G418) (Thermo Fisher Scientific) at 24 hpt, and the concentration of G418 was increased to 2,000 μg/ml at 48 hpt. Thereafter, cells were subcultured and maintained in culture medium supplemented with 400 μg/ml of G418. To establish a cell line continuously expressing SARS-CoV-2 N protein, HEK293 cells transfected with the pEB-SARS-CoV-2 N-His_{12} plasmid were selected by puromycin (2 μg/ml). For luciferase assays, Vero E6 cells were cotransfected with nLuc replicon plasmids and a promoterless plasmid pGL4.10 encoding firefly luciferase (Promega). In some experiments, plasmids expressing the N protein or EGFPs were also included in the cotransfection. At predetermined time points after transfection, cells were harvested and lysed with

passive lysis buffer (Promega). Luciferase assay was performed using the Nano-Glo dual-luciferase reporter assay system (Promega) in a GloMax 20/20 Luminometer according to the manufacturer's instructions. For each sample, nLuc activity was normalized to the fLuc reading or to the total protein concentration determined by a Bradford assay (Bio-Rad).

Generation of SARS-CoV-2 N protein antisera. We used a DNA prime-protein boost strategy to generate SARS-CoV-2 N antibodies. For this purpose, plasmid pcDNA3-SARS-CoV-2 N-Flag was purified using the endo-free Maxi plasmid extraction kit (Qiagen). His-tagged SARS-CoV-2 N protein was purified from the N-expressing cells using Ni-NTA agarose beads (Qiagen) and dialyzed against sterile phosphate-buffered saline (PBS) using Slide-A-Lyzer dialysis cassettes (Thermo Fisher Scientific). Two rabbits were intradermally injected with pcDNA3-SARS-CoV-2 N plasmid (500 μg per animal) twice with a 21-day interval. Each rabbit was boosted by subcutaneously injecting with 10 μg of purified SARS-CoV-2 N protein formulated with TiterMax Gold adjuvant (MilliporeSigma) twice at 42 and 63 days after primary immunization, respectively. Serum samples were collected prior to primary immunization and at 3 weeks after the last immunization. Antibody titers were determined by ELISA.

ELISA. Clear round-bottom Immuno nonsterile 96-well plates (Thermo Fisher Scientific) were coated overnight at 4°C with 100 μl of purified SARS-CoV-2 N protein (5 μg/ml). The plates were blocked with 200 μl of 5% skim milk in PBS containing 0.1% (vol/vol) Tween 20 (PBS-T) for 1 h at room temperature. Subsequently, 100 μl of 2-fold-diluted rabbit anti-SARS-CoV-2 N sera was added to the coated wells, followed by incubation for 1 h. Peroxidase-labeled donkey anti-rabbit Ig (Amersham Biosciences) was then added, followed by incubation for 1 h. The plates were washed five times with PBS-T between the incubation steps. Finally, SIGMA*FAST* OPD (Sigma) was added for color development, and the absorbance was measured at 450 nm using a SpectraMax microplate reader (Molecular Devices).

Western blotting and antibodies. Cell lysates were subjected to 10% sodium dodecyl sulfate-polyacrylamide gel electrophoresis (SDS-PAGE) and transferred onto nitrocellulose membranes (Millipore). The membranes were blocked with 5% skim milk in PBS-T overnight at 4°C, followed by incubation with a primary antibody for 2 h at room temperature. After three washes with PBS-T, the membranes were subsequently incubated with the appropriate infrared dye-labeled secondary antibodies (Li-Cor Biosciences) for 1 h at room temperature, followed by five washes with PBS-T before being scanned with Odyssey CLx imaging system (Li-Cor Biosciences). Rabbit anti-SARS-CoV-2 N was generated in-house as described above; Flag tag and β-actin antibodies were purchased from Cell Signaling Technology. The secondary antibodies IRDye 680 goat anti-rabbit IgG and IRDye 800 CW goat anti-mouse IgG were purchased from Li-Cor Biosciences.

RNA extraction and quantitative real-time PCR analyses. Total RNA was extracted from transfected Vero E6 cells using RNeasy minikit (Qiagen). RNA samples were treated with DNase I (Thermo Fisher Scientific) and reverse transcribed into cDNA using iScript cDNA synthesis kit (Bio-Rad). RT-qPCR was performed in an iQ5 real-time PCR detection system (Bio-Rad) using the SsoAdvanced Universal SYBR Green Supermix (Bio-Rad) with primers listed in Table 2. The RNA levels of target genes were normalized to that of glyceraldehyde-3-phosphate dehydrogenase (GAPDH). The relative expression levels were determined by the $2^{-\Delta\Delta CT}$ method (57).

Immunofluorescence staining. Vero E6 cells were cultured in a chamber slide and transfected with vector or the pSARS-CoV-2-Rep construct. The cells were harvested at 48 hpt, fixed with 4% paraformaldehyde for 20 min, treated with 0.1% glycine in PBS for 5 min, permeabilized with 0.1% Triton X-100 in PBS-T for 10 min, and blocked with 5% bovine serum albumin in PBS for 1 h at room temperature. Subsequently, the cells were incubated with rabbit anti-SARS-CoV-2 N antibody at 4°C overnight, and goat anti-rabbit IgG(H+L) highly cross-adsorbed secondary antibody, labeled with Alexa Fluor 594 (Thermo Fisher Scientific), was added at room temperature for 1 h. Finally, the cell nuclei were stained with 300 nM (4′,6′-diamidino-2-phenylindole; Sigma) for 10 min. After a washing step, the slides were mounted in ProLong Diamond Antifade Mountant (Thermo Fisher Scientific), covered with coverslips, and dried in the dark for 24 h. Cell images were collected by using a fluorescence microscope with appropriate settings (Zeiss Axioplan 2).

Antiviral assay. Vero E6 cells were cultured in 24-well plates and cotransfected with 250 ng of pSARS-CoV-2-nLuc-Rep replicon and 250 ng of pGL4.10. At 12 hpt, the cells were treated with 5, 10, or 20 μM remdesivir or the same volume of diluent DMSO. Cells were harvested at 24 or 48 h after treatment for luciferase analysis.

Statistical analysis. All experiments were performed in triplicates, and data are expressed as means $\pm$ the standard deviations. Data analysis was performed using GraphPad Prism7, and statistical differences were determined by using a Student *t* test or one-way analysis of variance (ANOVA), followed by Turkey's multiple comparisons. Comparisons of mRNA levels between groups were performed using one-way ANOVA with the Dunnett *post hoc* test. Statistical significance is indicated in the figures (*, $P < 0.05$; **, $P < 0.01$; ***, $P < 0.001$; ****, $P < 0.0001$; NS, not significant).

ACKNOWLEDGMENTS

We thank the animal care staff at VIDO for their assistance in generating antisera against SARS-CoV-2 N protein. We also thank Mingmin Liao and Ken Lai for their help.

This study was supported by grants from the Canadian Institutes of Health Research (DC0190GP), the Saskatchewan Agriculture Development Fund (20180101), the Natural Sciences and Engineering Research Council of Canada (RGPIN-2018-

04138), and VIDO. This article is published with the permission of the Director of VIDO, journal series no. 929.

REFERENCES

1. Rodriguez M, Soler Y, Perry M, Reynolds JL, El-Hage N. 2020. Impact of severe acute respiratory syndrome coronavirus 2 (SARS-CoV-2) in the nervous system: implications of COVID-19 in neurodegeneration. Front Neurol 11:583459. https://doi.org/10.3389/fneur.2020.583459.
2. Bos R, Rutten L, van der Lubbe JEM, Bakkers MJG, Hardenberg G, Wegmann F, Zuijdgeest D, de Wilde AH, Koornneef A, Verwilligen A, van Manen D, Kwaks T, Vogels R, Dalebout TJ, Myeni SK, Kikkert M, Snijder EJ, Li Z, Barouch DH, Vellinga J, Langedijk JPM, Zahn RC, Custers J, Schuitemaker H. 2020. Ad26 vector-based COVID-19 vaccine encoding a prefusion-stabilized SARS-CoV-2 Spike immunogen induces potent humoral and cellular immune responses. NPJ Vaccines 5:91. https://doi.org/10.1038/s41541-020-00243-x.
3. Xie X, Muruato A, Lokugamage KG, Narayanan K, Zhang X, Zou J, Liu J, Schindewolf C, Bopp NE, Aguilar PV, Plante KS, Weaver SC, Makino S, LeDuc JW, Menachery VD, Shi P-Y. 2020. An infectious cDNA clone of SARS-CoV-2. Cell Host Microbe 27:841–848 e3. https://doi.org/10.1016/j.chom.2020.04.004.
4. Hazarika BB, Gupta D. 2020. Modelling and forecasting of COVID-19 spread using wavelet-coupled random vector functional link networks. Appl Soft Comput 96:106626. https://doi.org/10.1016/j.asoc.2020.106626.
5. Abuo-Rahma GE-DA, Mohamed MFA, Ibrahim TS, Shoman ME, Samir E, Abd El-Baky RM. 2020. Potential repurposed SARS-CoV-2 (COVID-19) infection drugs. RSC Adv 10:26895–26916. https://doi.org/10.1039/D0RA05821A.
6. Khailany RA, Safdar M, Ozaslan M. 2020. Genomic characterization of a novel SARS-CoV-2. Gene Rep 19:100682. https://doi.org/10.1016/j.genrep.2020.100682.
7. Khan SA, Zia K, Ashraf S, Uddin R, Ul-Haq Z. 2020. Identification of chymotrypsin-like protease inhibitors of SARS-CoV-2 via integrated computational approach. J Biomol Struct Dyn 39:2607–2616. https://doi.org/10.1080/07391102.2020.1751298.
8. Toyoshima Y, Nemoto K, Matsumoto S, Nakamura Y, Kiyotani K. 2020. SARS-CoV-2 genomic variations associated with mortality rate of COVID-19. J Hum Genet 65:1075–1082. https://doi.org/10.1038/s10038-020-0808-9.
9. Subissi L, Posthuma CC, Collet A, Zevenhoven-Dobbe JC, Gorbalenya AE, Decroly E, Snijder EJ, Canard B, Imbert I. 2014. One severe acute respiratory syndrome coronavirus protein complex integrates processive RNA polymerase and exonuclease activities. Proc Natl Acad Sci U S A 111:E3900–E3909. https://doi.org/10.1073/pnas.1323705111.
10. Almazan F, Galan C, Enjuanes L. 2004. The nucleoprotein is required for efficient coronavirus genome replication. J Virol 78:12683–12688. https://doi.org/10.1128/JVI.78.22.12683-12688.2004.
11. Zuniga S, Cruz JLG, Sola I, Mateos-Gomez PA, Palacio L, Enjuanes L. 2010. Coronavirus nucleocapsid protein facilitates template switching and is required for efficient transcription. J Virol 84:2169–2175. https://doi.org/10.1128/JVI.02011-09.
12. Ashour HM, Elkhatib WF, Rahman MM, Elshabrawy HA. 2020. Insights into the recent 2019 novel coronavirus (SARS-CoV-2) in light of past human coronavirus outbreaks. Pathogens 9:186. https://doi.org/10.3390/pathogens9030186.
13. Grifoni A, Sidney J, Zhang Y, Scheuermann RH, Peters B, Sette A. 2020. A sequence homology and bioinformatic approach can predict candidate targets for immune responses to SARS-CoV-2. Cell Host Microbe 27:671–680 e2. https://doi.org/10.1016/j.chom.2020.03.002.
14. Zakhartchouk AN, Viswanathan S, Mahony JB, Gauldie J, Babiuk LA. 2005. Severe acute respiratory syndrome coronavirus nucleocapsid protein expressed by an adenovirus vector is phosphorylated and immunogenic in mice. J Gen Virol 86:211–215. https://doi.org/10.1099/vir.0.80530-0.
15. Kumar J, Qureshi R, Sagurthi SR, Qureshi IA. 2021. Designing of nucleocapsid protein based novel multi-epitope vaccine against SARS-CoV-2 using immunoinformatics approach. Int J Pept Res Ther 27:941–916. https://doi.org/10.1007/s10989-020-10140-5.
16. Kwarteng A, Asiedu E, Sakyi SA, Asiedu SO. 2020. Targeting the SARS-CoV2 nucleocapsid protein for potential therapeutics using immunoinformatics and structure-based drug discovery techniques. Biomed Pharmacother 132:110914. https://doi.org/10.1016/j.biopha.2020.110914.
17. Oliveira SC, de Magalhaes MTQ, Homan EJ. 2020. Immunoinformatic analysis of SARS-CoV-2 nucleocapsid protein and identification of COVID-19 vaccine targets. Front Immunol 11:587615. https://doi.org/10.3389/fimmu.2020.587615.
18. Deng X, Baker SC. 2018. An "old" protein with a new story: coronavirus endoribonuclease is important for evading host antiviral defenses. Virology 517:157–163. https://doi.org/10.1016/j.virol.2017.12.024.
19. Gordon DE, Jang GM, Bouhaddou M, Xu J, Obernier K, White KM, O'Meara MJ, Rezelj VV, Guo JZ, Swaney DL, Tummino TA, Hüttenhain R, Kaake RM, Richards AL, Tutuncuoglu B, Foussard H, Batra J, Haas K, Modak M, Kim M, Haas P, Polacco BJ, Braberg H, Fabius JM, Eckhardt M, Soucheray M, Bennett MJ, Cakir M, McGregor MJ, Li Q, Meyer B, Roesch F, Vallet T, Mac Kain A, Miorin L, Moreno E, Naing ZZC, Zhou Y, Peng S, Shi Y, Zhang Z, Shen W, Kirby IT, Melnyk JE, Chorba JS, Lou K, Dai SA, Barrio-Hernandez I, Memon D, Hernandez-Armenta C, et al. 2020. A SARS-CoV-2 protein interaction map reveals targets for drug repurposing. Nature 583:459–468. https://doi.org/10.1038/s41586-020-2286-9.
20. Kim Y, Jedrzejczak R, Maltseva NI, Wilamowski M, Endres M, Godzik A, Michalska K, Joachimiak A. 2020. Crystal structure of nsp15 endoribonuclease NendoU from SARS-CoV-2. Protein Sci 29:1596–1605. https://doi.org/10.1002/pro.3873.
21. Kindler E, Gil-Cruz C, Spanier J, Li Y, Wilhelm J, Rabouw HH, Züst R, Hwang M, V'kovski P, Stalder H, Marti S, Habjan M, Cervantes-Barragan L, Elliot R, Karl N, Gaughan C, van Kuppeveld FJM, Silverman RH, Keller M, Ludewig B, Bergmann CC, Ziebuhr J, Weiss SR, Kalinke U, Thiel V. 2017. Early endonuclease-mediated evasion of RNA sensing ensures efficient coronavirus replication. PLoS Pathog 13:e1006195. https://doi.org/10.1371/journal.ppat.1006195.
22. Kang H, Bhardwaj K, Li Y, Palaninathan S, Sacchettini J, Guarino L, Leibowitz JL, Kao CC. 2007. Biochemical and genetic analyses of murine hepatitis virus nsp15 endoribonuclease. J Virol 81:13587–13597. https://doi.org/10.1128/JVI.00547-07.
23. Deng X, Hackbart M, Mettelman RC, O'Brien A, Mielech AM, Yi G, Kao CC, Baker SC. 2017. Coronavirus nonstructural protein 15 mediates evasion of dsRNA sensors and limits apoptosis in macrophages. Proc Natl Acad Sci U S A 114:E4251–E4260. https://doi.org/10.1073/pnas.1618310114.
24. Zhao J, Sun L, Zhao Y, Feng D, Cheng J, Zhang G. 2021. Coronavirus endoribonuclease ensures efficient viral replication and prevents protein kinase R activation. J Virol 95:e02103-20. https://doi.org/10.1128/JVI.02103-20.
25. Gao B, Gong X, Fang S, Weng W, Wang H, Chu H, Sun Y, Meng C, Tan L, Song C, Qiu X, Liu W, Forlenza M, Ding C, Liao Y. 2021. Inhibition of anti-viral stress granule formation by coronavirus endoribonuclease nsp15 ensures efficient virus replication. PLoS Pathog 17:e1008690. https://doi.org/10.1371/journal.ppat.1008690.
26. Ivanov KA, Hertzig T, Rozanov M, Bayer S, Thiel V, Gorbalenya AE, Ziebuhr J. 2004. Major genetic marker of nidoviruses encodes a replicative endoribonuclease. Proc Natl Acad Sci U S A 101:12694–12699. https://doi.org/10.1073/pnas.0403127101.
27. Almazan F, DeDiego ML, Galan C, Alvarez C, Enjuanes L. 2006. Identification of essential genes as a strategy to select a SARS candidate vaccine using a SARS-CoV infectious cDNA. Adv Exp Med Biol 581:579–583. https://doi.org/10.1007/978-0-387-33012-9_105.
28. Almazan F, DeDiego ML, Galan C, et al. 2006. Construction of a severe acute respiratory syndrome coronavirus infectious cDNA clone and a replicon to study coronavirus RNA synthesis. J Virol 80:10900–10906. https://doi.org/10.1128/JVI.00385-06.
29. Thi Nhu Thao T, Labroussaa F, Ebert N, V'kovski P, Stalder H, Portmann J, Kelly J, Steiner S, Holwerda M, Kratzel A, Gultom M, Schmied K, Laloli L, Hüsser L, Wider M, Pfaender S, Hirt D, Cippà V, Crespo-Pomar S, Schröder S, Muth D, Niemeyer D, Corman VM, Müller MA, Drosten C, Dijkman R, Jores J, Thiel V. 2020. Rapid reconstruction of SARS-CoV-2 using a synthetic genomics platform. Nature 582:561–565. https://doi.org/10.1038/s41586-020-2294-9.
30. Ogando NS, Zevenhoven-Dobbe JC, van der Meer Y, Bredenbeek PJ, Posthuma CC, Snijder EJ. 2020. The enzymatic activity of the nsp14 exoribonuclease is critical for replication of MERS-CoV and SARS-CoV-2. J Virol 94. https://doi.org/10.1128/JVI.01246-20.

31. Xia H, Cao Z, Xie X, Zhang X, Chen JY-C, Wang H, Menachery VD, Rajsbaum R, Shi P-Y. 2020. Evasion of type I interferon by SARS-CoV-2. Cell Rep 33:108234. https://doi.org/10.1016/j.celrep.2020.108234.
32. Shizuya H, Birren B, Kim UJ, Mancino V, Slepak T, Tachiiri Y, Simon M. 1992. Cloning and stable maintenance of 300-kilobase-pair fragments of human DNA in *Escherichia coli* using an F-factor-based vector. Proc Natl Acad Sci U S A 89:8794–8797. https://doi.org/10.1073/pnas.89.18.8794.
33. Almazan F, Sola I, Zuniga S, Marquez-Jurado S, et al. 2014. Coronavirus reverse genetic systems: infectious clones and replicons. Virus Res 189:262–270. https://doi.org/10.1016/j.virusres.2014.05.026.
34. Liu MA. 2019. A comparison of plasmid DNA and mRNA as vaccine technologies. Vaccines 7:37. https://doi.org/10.3390/vaccines7020037.
35. Almazan F, Gonzalez JM, Penzes Z, Izeta A, Calvo E, Plana-Duran J, Enjuanes L. 2000. Engineering the largest RNA virus genome as an infectious bacterial artificial chromosome. Proc Natl Acad Sci U S A 97:5516–5521. https://doi.org/10.1073/pnas.97.10.5516.
36. Ye C, Chiem K, Park J-G, Oladunni F, Platt RN, Anderson T, Almazan F, de la Torre JC, Martinez-Sobrido L. 2020. Rescue of SARS-CoV-2 from a single bacterial artificial chromosome. mBio 11. https://doi.org/10.1128/mBio.02168-20.
37. Almazan F, Marquez-Jurado S, Nogales A, Enjuanes L. 2015. Engineering infectious cDNAs of coronavirus as bacterial artificial chromosomes. Methods Mol Biol 1282:135–152. https://doi.org/10.1007/978-1-4939-2438-7_13.
38. Rihn SJ, Merits A, Bakshi S, Turnbull ML, Wickenhagen A, Alexander AJT, Baillie C, Brennan B, Brown F, Brunker K, Bryden SR, Burness KA, Carmichael S, Cole SJ, Cowton VM, Davies P, Davis C, De Lorenzo G, Donald CL, Dorward M, Dunlop JI, Elliott M, Fares M, da Silva Filipe A, Freitas JR, Furnon W, Gestuveo RJ, Geyer A, Giesel D, Goldfarb DM, Goodman N, Gunson R, Hastie CJ, Herder V, Hughes J, Johnson C, Johnson N, Kohl A, Kerr K, Leech H, Lello LS, Li K, Lieber G, Liu X, Lingala R, Loney C, Mair D, McElwee MJ, McFarlane S, Nichols J, et al. 2021. A plasmid DNA-launched SARS-CoV-2 reverse genetics system and coronavirus toolkit for COVID-19 research. PLoS Biol 19:e3001091. https://doi.org/10.1371/journal.pbio.3001091.
39. Wang B, et al. Zhang C, Lei X, Ren L, Zhao Z, Huang H. 2021. Construction of non-infectious SARS-CoV-2 replicons and their application in drug evaluation. Virol Sin https://doi.org/10.1007/s12250-021-00369-9.
40. Dai W, Zhang B, Jiang X-M, Su H, Li J, Zhao Y, Xie X, Jin Z, Peng J, Liu F, Li C, Li Y, Bai F, Wang H, Cheng X, Cen X, Hu S, Yang X, Wang J, Liu X, Xiao G, Jiang H, Rao Z, Zhang L-K, Xu Y, Yang H, Liu H. 2020. Structure-based design of antiviral drug candidates targeting the SARS-CoV-2 main protease. Science 368:1331–1335. https://doi.org/10.1126/science.abb4489.
41. Touret F, Gilles M, Barral K, Nougairède A, van Helden J, Decroly E, de Lamballerie X, Coutard B. 2020. *In vitro* screening of an FDA-approved chemical library reveals potential inhibitors of SARS-CoV-2 replication. Sci Rep 10:13093. https://doi.org/10.1038/s41598-020-70143-6.
42. Wang JM, Wang LF, Shi ZL. 2008. Construction of a non-infectious SARS coronavirus replicon for application in drug screening and analysis of viral protein function. Biochem Biophys Res Commun 374:138–142. https://doi.org/10.1016/j.bbrc.2008.06.129.
43. Ge F, Luo Y, Liew PX, Hung E. 2007. Derivation of a novel SARS-coronavirus replicon cell line and its application for anti-SARS drug screening. Virology 360:150–158. https://doi.org/10.1016/j.virol.2006.10.016.
44. Krishnan DA, Sangeetha G, Vajravijayan S, Nandhagopal N, Gunasekaran K. 2020. Structure-based drug designing towards the identification of potential anti-viral for COVID-19 by targeting endoribonuclease NSP15. Inform Med Unlocked 20:100392. https://doi.org/10.1016/j.imu.2020.100392.
45. McBride R, van Zyl M, Fielding BC. 2014. The coronavirus nucleocapsid is a multifunctional protein. Viruses 6:2991–3018. https://doi.org/10.3390/v6082991.
46. Pruijssers AJ, George AS, Schäfer A, Leist SR, Gralinksi LE, Dinnon KH, Yount BL, Agostini ML, Stevens LJ, Chappell JD, Lu X, Hughes TM, Gully K, Martinez DR, Brown AJ, Graham RL, Perry JK, Du Pont V, Pitts J, Ma B, Babusis D, Murakami E, Feng JY, Bilello JP, Porter DP, Cihlar T, Baric RS, Denison MR, Sheahan TP. 2020. Remdesivir inhibits SARS-CoV-2 in human lung cells and chimeric SARS-CoV expressing the SARS-CoV-2 RNA polymerase in mice. Cell Rep 32:107940. https://doi.org/10.1016/j.celrep.2020.107940.
47. Rubin D, Chan-Tack K, Farley J, Sherwat A. 2020. FDA approval of remdesivir: a step in the right direction. N Engl J Med 383:2598–2600. https://doi.org/10.1056/NEJMp2032369.
48. Hackbart M, Deng X, Baker SC. 2020. Coronavirus endoribonuclease targets viral polyuridine sequences to evade activating host sensors. Proc Natl Acad Sci U S A 117:8094–8103. https://doi.org/10.1073/pnas.1921485117.
49. Kumar S, Kashyap P, Chowdhury S, Kumar S, Panwar A, Kumar A. 2021. Identification of phytochemicals as potential therapeutic agents that binds to nsp15 protein target of coronavirus (SARS-CoV-2) that are capable of inhibiting virus replication. Phytomedicine 85:153317. https://doi.org/10.1016/j.phymed.2020.153317.
50. Khan RJ, Jha RK, Singh E, Jain M, Amera GM, et al. 2020. Identification of promising antiviral drug candidates against nonstructural protein 15 (NSP15) from SARS-CoV-2: an *in silico* assisted drug-repurposing study. J Biomol Struct Dyn 2020:1–11.
51. Shi J, Zhang H, Fang L, Xi Y, Zhou Y, Luo R, Wang D, Xiao S, Chen H. 2014. A novel firefly luciferase biosensor enhances the detection of apoptosis induced by ESAT-6 family proteins of *Mycobacterium tuberculosis*. Biochem Biophys Res Commun 452:1046–1053. https://doi.org/10.1016/j.bbrc.2014.09.047.
52. Brown AJ, Won JJ, Graham RL, Dinnon KH, Sims AC, Feng JY, Cihlar T, Denison MR, Baric RS, Sheahan TP. 2019. Broad spectrum antiviral remdesivir inhibits human endemic and zoonotic deltacoronaviruses with a highly divergent RNA dependent RNA polymerase. Antiviral Res 169:104541. https://doi.org/10.1016/j.antiviral.2019.104541.
53. Sheahan TP, Sims AC, Graham RL, Menachery VD, Gralinski LE, et al. 2017. Broad-spectrum antiviral GS-5734 inhibits both epidemic and zoonotic coronaviruses. Sci Transl Med 9:eaal3653. https://doi.org/10.1126/scitranslmed.aal3653.
54. de Wit E, Feldmann F, Cronin J, Jordan R, Okumura A, Thomas T, Scott D, Cihlar T, Feldmann H. 2020. Prophylactic and therapeutic remdesivir (GS-5734) treatment in the rhesus macaque model of MERS-CoV infection. Proc Natl Acad Sci U S A 117:6771–6776. https://doi.org/10.1073/pnas.1922083117.
55. Hirotsu Y, Mochizuki H, Omata M. 2020. Double-quencher probes improve detection sensitivity toward severe acute respiratory syndrome coronavirus 2 (SARS-CoV-2) in a reverse-transcription polymerase chain reaction (RT-PCR) assay. J Virol Methods 284:113926. https://doi.org/10.1016/j.jviromet.2020.113926.
56. Wang D, Fang L, Shi Y, Zhang H, Gao L, Peng G, Chen H, Li K, Xiao S. 2016. Porcine epidemic diarrhea virus 3C-like protease regulates its interferon antagonism by cleaving NEMO. J Virol 90:2090–2101. https://doi.org/10.1128/JVI.02514-15.
57. Livak KJ, Schmittgen TD. 2001. Analysis of relative gene expression data using real-time quantitative PCR and the $2^{-\Delta\Delta CT}$ method. Methods 25:402–408. https://doi.org/10.1006/meth.2001.1262.